Metallomics

Differential translational control of 5' IRE-containing mRNA in response to dietary iron deficiency and acute iron overload

Journal:	*Metallomics*
Manuscript ID	MT-ART-08-2020-000192.R1
Article Type:	Paper
Date Submitted by the Author:	30-Oct-2020
Complete List of Authors:	Garza, Kerry; MediTech Media Clarke, Stephen; Oklahoma State University Stillwater, Nutritional Sciences Ho, Yi-Hsuan; Hologic Inc Bruss, Matthew; Exploration Academy Vasanthakumar, Aparna; AbbVie Inc Anderson, Sheila; University of Wisconsin-Madison, Nutritional Sciences Eisenstein, Richard; University of Wisconsin-Madison, Nutritional Sciences

SIGNIFICANCE TO METALLOMICS

Iron is a common cofactor for proteins in many organisms. Iron regulatory proteins (IRP[1]) iron-regulated RNA binding proteins that are essential participants in the response of animal cells to changes in iron availability. IRP control the fate of mRNA encoding proteins regulating cellular iron metabolism or the responses to iron deficiency. Although the targeted mRNA encode proteins of widely different roles in cellular function the extent to which they are hierarchically regulated by IRP is not clear. Our analysis describes an iron-dependent translational regulatory hierarchy of IRP targeted mRNAs that facilitates the adaptive responses to iron deficiency or excess.

[1] Abbreviations: AC, ammonium citrate; C, control; c-acon, cytosolic aconitase; CS, citrate synthase; eALAS, erythroid 5-aminolevulinate synthase; EMSA, electrophoretic mobility shift assay, FAC, ferric ammonium citrate; Fpn, ferroportin; Ftn, ferritin; m-acon, mitochondrial aconitase; HIF-2α, hypoxia inducible factor 2α; HHCS, hyperferritinemia cataract syndrome; ID, iron deficient; IRE, iron responsive element; IRP, iron regulatory protein; RNP, ribonucleoprotein particle; TfR, transferrin receptor; Tth, transthyretin; UTR, untranslated region.

Differential translational control of 5' IRE-containing mRNA in response to dietary iron deficiency and acute iron overload

Kerry L. Garza[a†], Stephen L. Clarke[b†], Yi-Hsuan Ho[c], Matthew D. Bruss[d], Aparna Vasanthakumar[e], Sheila A. Anderson, and Richard S. Eisenstein

University of Wisconsin

Department of Nutritional Sciences

Madison, WI 53706

United States of America.

ABSTRACT

Iron regulatory proteins (IRPs) are iron-responsive RNA binding proteins that dictate changes in cellular iron metabolism in animal cells by controlling the fate of mRNAs containing iron responsive elements (IREs). IRPs have broader physiological roles as some targeted mRNAs encode proteins with functions beyond iron metabolism suggesting hierarchical regulation of IRP-targeted mRNAs. We observe that the translational regulation of IRP-targeted mRNAs encoding iron storage (L- and H-ferritins) and export (ferroportin) proteins have different set-points of iron responsiveness compared to that for the TCA cycle enzyme mitochondrial aconitase. The ferritins and ferroportin mRNA were largely translationally repressed in liver of rats fed a normal diet whereas mitochondrial aconitase mRNA is primarily polysome bound. Consequently, acute iron overload increases polysome association of H- and L-ferritin and ferroportin mRNAs while mitochondrial aconitase mRNA showed little stimulation. Conversely, mitochondrial aconitase mRNA is most responsive in iron deficiency. These differences in regulation were associated with a faster off-rate of IRP1 for the IRE of mitochondrial aconitase in comparison to that of L-ferritin. Thus, hierarchical control of mRNA translation by IRPs involves selective control of cellular functions acting at

different states of cellular iron status and that are critical for adaptations to iron deficiency or prevention of iron toxicity.

INTRODUCTION

Sensory and regulatory mechanisms utilizing RNA-based control form essential homeostatic networks in prokaryotes and eukaryotes (1-4). RNA binding proteins, non-coding RNAs and mRNA targets form RNA regulons that coordinate fundamental cellular processes such as growth control and whose dysregulation is associated with common human diseases including oncogenesis (1). IRPs are iron-regulated RNA binding proteins that sense cellular iron levels and control the fate of mRNAs essential for the maintenance of metazoan iron homeostasis in diverse physiological scenarios (3,5). IRPs bind stem-loop structures termed iron responsive elements (IREs) in the untranslated regions (UTR) of mRNA encoding proteins required for controlling the uptake and metabolic fate of iron, the adaptive responses to iron deficiency and other physiological processes. IRPs directly control mRNA translation or stability depending on the location of the IRE. The first identified targets of IRP action are the mRNA encoding the H- and L-subunits of the iron storage protein ferritin (FTH1 and FTL) and the iron uptake protein transferrin receptor 1 (TFRC). IRPs bind to the single IRE near the 5′ end of ferritin mRNA and block an early step in the initiation phase of translation (6). In contrast, IRPs bind to multiple IREs in the 3' UTR of *Tfrc* mRNA where they promote its stabilization. To date functional IREs have been identified in ten mRNA, and

transcriptomic studies suggest that IRPs may control a much broader post-transcriptional regulon (3,7-9). Several of the more recently identified IRE-containing mRNAs encode proteins without direct roles in iron metabolism and for some mRNA IRPs have been proposed to interact with sequences lacking the canonical IRE structure (3,7,8,10). The breadth of the cellular processes controlled by proteins encoded by mRNA with established functional IRE(s) suggests that IRPs differentially regulate mRNA fate (5,11). However, it has not been determined if iron-dependent control of IRP action allows for selective control of proteins directly involved in iron metabolism versus proteins needed for adaptive changes in cellular function.

Identification of a functional IRE in the 5' UTR of the tricarboxylic cycle enzyme mitochondrial aconitase (*Aco2*) mRNA provided the first indication that the physiological action of IRPs extended beyond the direct control of the uptake and metabolic fate of iron (12,13). IRE-containing mRNAs encoding proteins involved in cell cycle regulation (CDC14A) and oxygen-sensing (HIF-2 α; EPAS1) were then identified, further expanding the range and organismal roles of the IRP RNA regulon (14,15). Subsequently, a transcriptome-wide approach identified a broad array of potential IRP mRNA targets which led to the recent demonstration of the unanticipated role of the actin binding protein profilin 2 (PFN2) in iron metabolism (8). These findings support the

concept that the iron-dependent control of mRNA fate by IRPs may be separable into primary targets required for the maintenance of cellular iron homeostasis and secondary targets involving proteins that mediate adaptive changes in cellular pathways during stress such as those needed for cell survival in iron-deficient environments.

The functional impact of naturally occurring IRE mutations supports the concept that RNA binding hierarchy is a key factor allowing for selective action of IRPs. Many mutations in human *Ftl* IRE individually give rise to hereditary hyperferritinemia cataract syndrome (HHCS) and high serum ferritin (16-18). The severity of the disease phenotype in HHCS is strongly related to the extent to which these IRE mutations reduce IRP binding affinity and is directly related to the accumulation of serum ferritin, a likely measure of translational derepression of *Ftl* mRNA (16). The strongest increase in serum ferritin accumulation occurs over the first 10-fold decrement of IRE binding affinity; mutations that cause a greater loss of RNA binding showed a smaller relative increase in serum ferritin (16). Interestingly, the affinity with which IRP1 recognizes the six established 5' IREs varies over a 9-fold range (19). These differences in affinity of interaction of IRP1 with the known 5' IREs also supports the existence of an iron-dependent translational regulatory hierarchy essential for the maintenance of metazoan iron homeostasis.

The presence of 5' IRE in multiple mammalian mRNA encoding proteins of differing metabolic functions provides a means to determine the extent to which IRPs selectively determine mRNA fate. Several studies have demonstrated strong repression of ferritin subunit mRNA in animals or cell lines (20-23). In comparison, erythroid 5-aminolevulinate synthase (*Alas2*) and *Hif-2α* mRNAs are less strongly repressed *in vivo* (24-26), as is *Aco2* mRNA in a cell-free system (27). While these findings indicate that the translation of 5' IRE-containing mRNA is selectively regulated, the extent to which the set point may vary for iron regulation of the translation of these mRNA has not been determined. Furthermore, while results of previous studies support the existence of a translational regulon amongst IRE-containing mRNA (24), the full spectrum of iron-regulation of the translation by IRPs in a single physiological system has not been investigated. Whether this hierarchical mechanism can fully explain iron regulation of the steady-state level of proteins encoded by 5' IRE-containing mRNA is not clear.

In this study, we determined the impact of iron overload and iron deficiency on the translational regulation of multiple 5' IRE-containing mRNA in rat liver. Our results show that 5' IRE-containing mRNA encoding proteins that directly control cellular iron metabolism are more translationally repressed in normal liver and respond most strongly to iron overload. In contrast,

the 5' IRE-containing mRNA encoding *Aco2* mRNA is largely translated in normal liver and is most responsive to iron deficiency. We demonstrate that the IRE from a weak target, *Aco2* mRNA, dissociates from IRP1 much faster than does L-ferritin IRE suggesting enhanced access of *Aco2* mRNA to the translation machinery. Taken together, our results demonstrate that the iron-dependent regulation of 5' IRE-containing mRNA translation selectively controls pathways involved in the adaptive responses to iron deficiency and those required for survival in iron overload.

EXPERIMENTAL

Polysome profile analysis: A method similar to Anthony *et. al* was used (28). Livers were excised and washed in ice-cold polysome buffer (40 mM HEPES pH 7.4, 100 mM KCl, 5 mM $MgCl_2$, 2 mM citrate, and 1 mM DTT). The liver was minced into small (~0.25-0.5 cm^3) pieces and a representative mixture of pieces were homogenized in 3 volumes of polysome using a Potter Elvehjem homogenizer fitted with a teflon pestle. The homogenate was centrifuged at 5000 x *g* at 4 ^oC for 20 min. The upper 2/3 of supernatant was collected and nine volumes of supernatant were diluted with one volume detergent (10% sodium deoxycholate, 10% Triton X-100). After gentle mixing 500 μL of the sample was layered over an ice-cold 11 ml linear 15% to 60% sucrose

gradient, in PB. The samples were centrifuged at 180,000 x *g* in a Sorvall TH641 swinging bucket rotor for 2 h at 4 ^{o}C with slow braking. The gradients were fractionated on an ISCO model UA-6 gradient fractionator. The absorbance at 254 nm was continuously monitored and ten 1-min (~1.2 ml) fractions were collected and stored at –80 ^{o}C overnight. Total RNA was isolated from 500 μL of each gradient fraction using Trizol (ThermoFisher). The integrity and location in the gradient of the 18S and 28S rRNAs was determined by agarose gel electrophoresis. Using the image as a guide, it was determined that fractions 1-2 contained the free protein pool, some of the ribonucleoprotein particle (RNP) pool and a portion of the 40S ribosomal subunit; fractions 3-4 contained RNPs, both ribosomal subunits and the 80 S monosome; and fractions 5-10 contained the light and heavy polysomes. Since the sedimentation velocity of a translationally repressed RNA will vary depending on the size of the mRNA some repressed mRNA (RNP) may overlap with the ribosomal subunits or the 80S monosome. Hence finding an mRNA in the 40S or 80S region may indicate it is translationally repressed or it can also indicate it is on the pathway of translational initiation. RNA from each gradient was reverse-transcribed to synthesize total cDNA (Reverse Transcription System, Promega). The total amount of mRNA for m-acon, L-ferritin, citrate

synthase, and transthyretin in each gradient fraction was quantified by real time PCR with SYBR Green using a Roche Light Cycler. PCR product size was confirmed by agarose gel electrophoresis.

The sequence of the PCR primers used are: Rat *Fth1*, sense: 5′ TACCACCAGGACTCGG; anti-sense: 5′ GGAAGATTCGTCCACCTC; *Ftl*, sense, 5′-CACTTCTTCCGCGAATTG-3', anti-sense, 5′-TCAGAGTGAGGCGCTCAA-3'; *Fpn1*, Sense: 5′ TGGAAGCCCCTTGGA C; anti-sense:5′ CCAAAGACCGATTCTAGC; *Aco2*, sense, 5′-GATCCGAGCCACTATCGA-3', anti-sense, 5′-TGGATCAAAGTCCGATCG-3'; citrate synthase (*Cs*), sense, 5′-CACTCAACTCGGGACG -3', anti-sense, 5′-CCTCGACACTCCGAAC-3'; and transthyretin (*Ttr*), sense, 5′-GGCAGCCCTGCTGTCGAT-3', anti-sense, 5′-TGCTGTAGGAGTACGGGC-3'. The level of 18S ribosomal RNA was quantified using QuantumRNA Classic 18S primers (ThermoFisher).

Total RNA level by qPCR: A portion of the homogenate was used for quantification of mRNA abundance by qPCR. The level of expression of these mRNA was normalized to the concentration of 18S ribosomal RNA in each sample. RNA was extracted from liver homogenates using Trizol according to the manufacturer's directions. RNA integrity was confirmed as noted above.

Immunoblotting: FTL, FTH1 and ACO2 protein level was determined by immunoblotting. Liver homogenate was solubilized by diluting it to a final concentration of 1% Triton X-100 followed by incubation in ice for 10 min. Insoluble material was removed by centrifugation at 14,000 x *g* for 10 min at 4 ^{o}C. Then 5 or 50 μg of protein from the solubilized homogenate was denatured for 10 min in Laemmli's reducing sample buffer at 65 ^{o}C or 100 ^{o}C for m-acon and ferritin samples, respectively (29). Protein concentrations were determined using the bicinchronic acid (BCA) method (ThermoFisher). A 10% polyacrylamide-SDS gel was used for all immunoblotting except for ferritin where the Tricine-SDS buffer was used (29). After transfer to nitrocellulose (Schleicher and Schuell) proteins were detected with protein A-purified rabbit IgG against bovine heart m-acon and rat liver ferritin, respectively, followed by incubation with goat anti-rabbit IgG-horseradish peroxidase conjugate (Southern Biotech) (29) using SuperSignal (ThermoFisher). Immunoblots was quantified by densitometry. Examination of α-tubulin as a loading control revealed its abundance to be altered in iron deficient liver, so immunoblots were normalized to total protein load (results not shown).

Animal treatment: The use of animals was reviewed and approved by the Institutional Animal Care and Use Committee of the University of Wisconsin Research Animal Resource Center.

Study 1 - acute iron overload:. Adult male Sprague-Dawley rats weighing 167 ± 1.4 g were provided with the purified control (C) diet containing 50 mg Fe/kg diet for 5 to 6 days (29). Rats were injected with either 0.6 ml of 10 mg/ml ferric ammonium citrate (FAC) or 0.6 ml of 10 mg/ml ammonium citrate (AC) three hr prior to killing. FAC and AC were prepared in sterile 0.9% NaCl with a final pH of 7.4. At termination rats in the control group weighed 221 ± 3 g (n = 3) while rats in the iron injected group weighed 219 ± 3 g (n = 3). A previous study using similar aged rats injected with a similar dose of iron per 100 g body weight found a 168% increase in total liver iron at 4 hr after injection (22).

Study 2 - iron deficiency without anemia. In this experiment weanling mice (21 d; 47 ± 1.1 g) were fed an iron adequate diet for 14 days to increase their iron stores before they were fed the C of iron-deficient (ID, < 2 mg Fe/kg diet) diet from the age of 35 to 49 days when they were considered adult age. At d 49 there was no difference in body weight in the control (223 ± 16) or ID (221 ± 7) groups. This approach allowed us to induce iron deficiency without anemia, in contrast to the approach in study 3 that produced rats with iron deficiency anemia.

Study 3 – iron deficiency with anemia. Weanling (21 d) male Sprague-Dawley rats weighing 45 ± 0.6 g were housed and fed either the C or ID diet for 7 to 9 days (d 28 – d 30 of age). Three rats from each diet group were killed and their livers were isolated for polysome profile analysis. At the end of the experimental period there was no significant difference in body weight of rats in the control (100 ± 2 g) or ID (90 ± 4 g) groups (mean ± SEM).

Blood analyses: Blood was collected from the inferior vena cava of the anesthesized rats after which livers were excised for polysome analysis. Hemoglobin (Hb) concentration was determined in heparinized blood (30). A portion of non-heparinized blood was used for preparing serum. Serum was used for the determination of percent transferrin saturation with iron, serum iron, and total iron binding capacity (Catalog # 565-A; Sigma).

RNA binding analyses: IRP RNA binding activity was determined using [^{32}P]rat *Ftl* IRE as described (19). Since both IRP1 and IRP2 regulate IRE-containing mRNA fate we report RNA binding activity as the summation of spontaneous RNA binding activity of IRP1 plus IRP2 in the as-isolated cytosol (i.e., without activation by 2-mercaptoethanol).

RNA dissociation from IRP1: Off-rate assays were performed using two approaches, electrophoretic mobility shift assay (EMSA) or nitrocellulose filter binding (31). Recombinant IRP1 was expressed in yeast, purified and the concentration of active IRP1 determined as described (31). [^{32}P]RNA was folded before the RNA binding assay as described (31). An IRP1:IRE complex was allowed to form using either 50 pM [^{32}P]*Ftl* IRE with 500 pM active IRP1 or 6 pM of [^{32}P]*Aco2* IRE with 130 pM active IRP1, incubated at 30°C for 10 min in binding buffer (5 mM DTT, 20 µg/ml nuclease-free BSA, 5% glycerol, 1mM magnesium acetate, 20 mM Hepes pH 7.5 and 75 mM potassium chloride). Higher amounts of IRP1 and IRE were used for the *Ftl* assay because the slower dissociation rate of this complex did allow for measurable amounts of free RNA if the lower concentration was used. Unlabeled competitor RNA was then added (25 nM *Ftl* IRE, UGUAUCUUGCUUCAACAGUGUUUGGACGGAACAGA; 1.3 nM *Aco2*, GCGACCUCAUCUUUGUCAGUGCACAAAAUGGCGCC, Dharmacon) and dissociation was allowed to occur at 30 °C. The amount of RNA-protein complex remaining was determined by EMSA or filter binding assay. Control experiments were carried out the same as described, except using anti-sense L-ferritin IRE, UCUGUUCCGUCCAAACACUGUUGAAGCAAGAUACA,

Dharmacon) as competitor RNA. Samples (30 µl) were withdrawn at specific time points and mixed with 3 µl of 0.5 mg/ml heparin and 25 µl of the mixture was loaded onto the gel with the current on at 90V. After all samples were loaded, the gel was run for 25 min at 250 V. Gels were loaded and run at 4°C to minimize dissociation of RNA from IRP1 during the run.

For the nitrocellulose filter binding assays samples were passed through nitrocellulose filters (Whatman, Protran BA85) that had been pre-wet with binding buffer (4°C) and incubated in buffer on ice until needed. Sample filtration was followed by addition of binding buffer (750 µl) at 4°C. The entire process from loading the sample to the drying of the filter by vacuum took 75 sec. The filter was then placed in scintillation vials with addition of scintillation mixture for counting. The data were fit to an exponential decay curve using GraphPad software.

Statistical analysis: Differences between group means were determined by Student's T-test. Differences were considered significant at a $P < 0.05$.

RESULTS

Differential translational repression of 5' IRE-containing mRNA in liver: To determine the extent to which IRPs hierarchically control the translation state of IRE-containing mRNAs we first performed studies in rats fed an iron sufficient diet that were injected with ferric ammonium citrate (acute iron overload) or ammonium citrate (control). A typical liver polysome profile from control animals revealed that the majority (~80%) of liver ribosomes were present as polysomes (Fig. 1A). We determined the translation state of four 5' IRE-containing mRNA, those encoding *Fth1, Ftl, Fpn1* and *Aco2*, in liver of acutely iron overloaded or control rats. The non-IRE-containing mRNAs encoding *Tth* and *Cs* mRNAs served as controls.

Both *Tth* and *Cs* mRNAs were well translated in the control rats injected with ammonium citrate given that at least 80% of these mRNA was polysome associated (Fig. 1C and 1D, Table 1). In contrast, the translation state of each of the 5′ IRE mRNA examined was more highly repressed in control rats, although the degree of repression varied depending on the mRNA. In this context, repression refers to the extent to which a given mRNA is not associated with polysomes. *Fth1* and *Ftl* mRNAs were most strongly repressed with only 12% of each mRNA being polysome-associated (Fig. 1E and 1F; Table 1). On a fractional basis and using the percent of *Fth1* and *Ftl* mRNAs on

polysomes as the reference about 48% more *Fpn1* (17.8% *Fpn1* vs. 12% *Fth1* and *Ftl*) and 400% more *Aco2* mRNA (62% m-acon vs. 12% ferritin) was present in the polysome fractions in liver if rats fed the iron sufficient diet (Fig. 1G and 1H, Table 1). These differences in translation state of the *Fth1* and *Ftl*, *Fpn1* and *Aco2* mRNA suggest that IRPs variably repress the translation of 5′ IRE containing mRNAs in liver. While the degree of repression of *Fth1* and *Ftl* mRNAs in rat liver under control conditions was similar to our previous study in mice (24) both *Fpn1* and *Aco2* mRNAs were more highly repressed in rat liver, suggesting a relatively iron-deficient state compared to mice.

To determine if the difference in translation state of 5′ IRE-containing mRNA is due to selective repression by IRPs, the extent to which acute iron overload caused translational derepression was examined. Treatment with ferric ammonium citrate (Iron) for 3 hr reduced IRP RNA binding activity (IRP1 plus IRP2) from 38 $\pm$ 2 fmol/mg protein to 24 $\pm$ 4 fmol/mg protein ($P < 0.05$) as measured by quantitative EMSA (see Supplementary material) (19). Acute iron overload strongly activated the translation of ferritin mRNAs as 80% of *Fth1* and *Ftl* became polysome-associated, nearly a 7-fold increase relative to control (Fig. 1E and 1F). A similar response was observed for *Fpn1* mRNA where more than 85% of this RNA was found in the polysome region after iron treatment (Fig. 1G). Interestingly, even in the case of *Aco2* mRNA, iron significantly

enhanced polysome association such that 84% of the messenger was polysome-bound, indicating that the relatively small fraction (~20%) m-acon mRNA found in the RNP region in control liver is being actively repressed by IRPs (Fig. 1H). In contrast to the IRE-containing mRNA, acute iron overload was without effect on the translation state of *Tth* and *Cs* mRNA which supports the conclusion that the impact of iron on mRNA translation is specific to 5' IRE-containing mRNAs and that global changes in ribosome distribution are not occurring (Fig. 1C and 1D, Table 1). It is notable that even though iron substantially stimulated the translation of the IRE-containing mRNA examined, a small fraction of the population of each mRNA remained in the RNP pool. The fractional amount of RNP-associated mRNA in iron overloaded rats was highest for the *Fth1* and *Ftl* mRNAs and lowest for *Aco2* mRNA (Table 1). In summary, in adult rats fed a normal diet, 5' IRE-containing mRNAs encoding the iron metabolism proteins FTH1 and FTL and FPN1 were highly repressed such that acute iron overload substantially increased their polysome association, while the tricarboxylic acid cycle enzyme *Aco2* was largely polysome bound in control liver and consequently responded minimally to iron stimulation.

Differential impact of iron deficiency on repression of 5′-IRE mRNA: To investigate further the selective control of 5′ IRE mRNA translation, the physiological response to dietary iron deficiency was determined. Since hypoxia can influence IRP RNA binding activity (32-35) we used a feeding regimen that produced iron-deficiency without anemia. Weanling rats (d 21) were fed an iron sufficient diet for two weeks before dividing them into a control or iron deficient group fed the C or ID diet, respectively, for two additional weeks. On the day of the experiment blood hemoglobin level was not significantly different between the two dietary groups being 13.2 ± 0.9 g hemoglobin/dl in rats fed the iron sufficient control (C) diet and 11.1 ± 0.6 g hemoglobin/dl in rats fed the iron-deficient (ID) diet ($P > 0.05$). In contrast, the percent saturation of serum transferrin with iron was strongly reduced ($P < 0.0006$) in the ID rats (9.0 ± 1.7 %) versus the control rats (35.3 ± 1.8 %). Liver IRP RNA binding activity (IRP1 plus IRP2) determined by EMSA (not shown) was 1.5-fold higher ($P < 0.05$) in the ID group (124 ± 6 fmol/mg protein) compared to the control group (83 ± 7 fmol/mg protein) (see Supplementary material). Thus, this experimental model allowed examination of the impact of iron deficiency without anemia on the translation state of 5′-IRE mRNA in liver.

For the animals fed the control iron-adequate diet used in this study the relative translational activity of 5′-IRE mRNA exhibited the same differential pattern of repression as noted in a previous study in mice (24) and is consistent with the range of binding affinities previously determined for all 5' IREs (19). *Ftl* mRNA was most extensively repressed followed by *Fpn1* and then *Aco2* mRNAs (Fig. 2C through 2E; Table 2). Iron deficiency resulted in a further repression of the translation of each of these mRNA. Polysomal-associated *Ftl* mRNA was most strongly affected exhibiting a 65% decrease in ID relative to C liver such that only 4% of *Ftl* mRNA appeared to be translationally active in iron deficient liver (Fig. 2C, Table 2). We also observed a 70% reduction in the total amount of *Ftl* mRNA in liver of the ID rats (Table 2). Iron is known to regulate *Ftl* gene transcription (22).

We also observed enhanced translational repression of other 5′-IRE mRNA albeit not to the extent to which *Ftl* mRNA responded. The relative translation rates of *Fpn1* and *Aco2* mRNA were more highly repressed in ID liver but the relative decline in their polysome association (~50%) was not as extensive as was the case for *Ftl* mRNA (Fig. 2). In iron-deficient liver, nearly 40% of *Aco2* mRNA remained polysome-associated, and this was more than 8-fold greater, on a fractional basis, than what was observed for *Ftl* (Fig. 2, compare panels C and E, Table 2). In the case of *Fpn1*,

nearly 4-fold more mRNA (17%), on a fractional basis, remained polysome-associated as compared to *Ftl* (Fig. 2, compare panels C and D). As noted in the first study the translational activity of *Tth* and *Cs* mRNAs was high, as 70 to 80% of these mRNA were polysome-associated (Fig. 2A and 2B, Table 2). While a significant decline in the total amount of these mRNA was noted in ID liver their relative abundance on polysomes, and hence their translational efficiency, was not affected by iron deficiency (Table 2).

The abundance of proteins encoded by mRNAs that are strongly (FTL) or weakly (ACO2) controlled by IRPs was differentially affected by iron deficiency. At the termination of this experiment the level of ACO2 or total ferritin (FTL and FTH1) protein in rats fed the control diet was not different compared to control rats killed on day zero (results not shown). However, total ferritin protein declined by 81% (Fig. 3) for rats fed the ID diet. In contrast, ACO2 protein level declined by 21% (Fig. 3). The more extensive decline in ferritin (FTL and FTH1) protein in iron-deficient liver reflects the stronger repression of its mRNA in response to dietary iron deficiency compared to other targets of IRP action.

Kinetics of IRP1:IRE dissociation contribute to differential translational regulation: The differential translational regulation of the *Ftl*, *Fpn1* and *Aco2* mRNAs fits well with our previous finding demonstrating that IRP1 binds to 5′-IRE in an RNA binding affinity hierarchy (19). To better understand the mechanistic basis for the selective translational regulation of 5′-IRE mRNA we determined the dissociation rate (k_{off}) for IRP1 when bound to *Ftl* or *Aco2* IRE. These IRE were chosen because they represent strongly versus weakly repressed mRNA and they display the largest (9-fold) difference in affinity for IRP1 (19,36). IRP1:[^{32}P]IRE complexes were allowed to form and the extent of RNA dissociation determined by gel shift or by nitrocellulose filter binding assay after addition of a 200-fold molar excess of competitor RNA. For each complex the specific competitor was an unlabeled version of the same IRE while the non-specific competitor was the antisense version of the *Ftl* IRE.

As determined by EMSA the amount of *Ftl* IRE- and Aco2 IRE-IRP1 complexes were stable in the absence of any RNA competitor (not shown) or in the presence of the non-specific competitor (Fig. 4C and 4F). However, when challenged with the unlabeled *Ftl* IRE, the [^{32}P]*Ftl* IRE-IRP1 complex dissociated with k_{-1} = 0.019 ± 0.0029 at 30° and a $t_{1/2}$ = 42.7 ± 7.9 min (mean ± SEM; n = 7) (Fig. 4A and 4C, Table 3). In contrast, the *Aco2* IRE:IRP1 complex dissociated

significantly more rapidly. When challenged with unlabeled *Aco2* IRE, the [^{32}P]*Aco2* IRE dissociated with k_{-1} = 0.13 ± 0.016 at 30° or a $t_{1/2}$ = 5.7 ± 0.8 min (mean ± SEM; n = 6) (Fig. 4D and F; Table 3). The off-rate for the *Aco2* IRE from IRP1 was 7.5-fold more rapid than was observed for the *Ftl* IRE. We also determined the off-rate for the *Aco2* and *Ftl* by nitrocellulose filter binding assay. A similar result was obtained as *Aco2* was found to dissociate nearly 6-fold more rapidly from IRP1 than was the case for the *Ftl* IRE (Table 3).

Iron-dependent control of ferritin protein level in the absence of translational control: It is well established that FPN1 and the FTH1 and FTL subunits, all encoded by 5' IRE-containing mRNA, are also strongly iron-regulated through targeted protein degradation mechanisms (37-39). In the case of ferritin, NCOA4 targets ferritin shells to the lysosome for degradation in the presence of iron (40). Our findings described below support the concept that iron-dependent control of ferritin protein stability provides an additional level of control that acts when translational repression is maximized. Weanling rats (d 21) were fed the ID or C diet for one week. Rats fed the ID diet were iron-deficient and anemic as indicated by their reduced blood hemoglobin concentration (7.7 ± 0.1 g/dL) relative to that observed in control rats (11.1 ± 0.3 g/dL) ($P < 0.05$). Similar to what was

observed in adults fed the control diet, only 10% of *Ftl* mRNA was polysome-associated in liver, and more than 70% of *Aco2* mRNA was in this fraction in weanling control rats (Fig. 5, Table 4). However, a different picture emerged in response to iron deficiency compared to what was observed in adult rats. Surprisingly the translation state of *Ftl* mRNA was not further repressed by iron deficiency (Fig. 5, Table 4) even though IRP RNA binding activity (IRP1 plus IRP2) increased from 80 $\pm$ 7 fmol/mg protein to 211 $\pm$ 12 fmol/mg protein ($P < 0.05$) (see Supplementary material). In contrast, translation of *Aco2* mRNAs was significantly repressed in iron-deficiency compared to liver from rats fed the control diet (Fig. 5E, Table 4). Iron-deficiency resulted in a 2.5-fold increase of *Aco2* mRNA in the RNP fraction, and a 37% decrease in the polysome fraction was observed relative to what was observed in liver of rats fed the iron sufficient diet (Fig. 5E, Table 4). *Fpn1* mRNA appeared to respond similarly to *Aco2* mRNA as the fraction of *Fpn1* mRNA that was polysome bound decreased from 29% to 17% (Fig. 5D, Table 4; n = 2). As was observed for adult rats, the translation state of *Tth* and *Cs* mRNA was unaffected by iron deficiency (Fig. 5A and 5B). Taken together, these results suggest that *Ftl* mRNA translation is maximally repressed in the liver of weanling rats fed an iron-adequate diet. In contrast, *Fpn1* and *Aco2* mRNA which are more

weakly repressed versus *Ftl* and *Fth1* mRNAs in rats fed a control diet, remained strongly responsive to iron deficiency even in weanling animals

We then asked if the different response of *Ftl* mRNA translation to iron deficiency in weanling rats relative to the adult rats used in our previous study was reflected at the protein level (Fig. 6). The 50% decline in ACO2 protein level in liver of weanling ID rats agreed well with previous observations (29) and is in line with the increased translational repression of this mRNA. Interestingly, ferritin protein (FTL and FTH1) level declined by 75% in the liver of ID weanling rats even though the translation state of *Ftl* mRNA was not altered relative to that observed in the liver of weanling rats fed an iron sufficient diet. Thus, substantial modulation of ferritin protein accumulation can occur in the absence of translational control of ferritin mRNA and this likely involves regulated changes in ferritin protein stability.

DISCUSSION

Our analyses of the impact of dietary iron deficiency and acute iron overload on a direct action of IRPs, the translational control of 5′ IRE-containing mRNA, support novel conclusions concerning how mammalians cells coordinate the modulation of cellular iron metabolism with

control of pathways involved in the adaptive response to iron deficiency (i.e. citrate metabolism). First, the different set-points for translational control of 5' IRE-containing mRNA observed here supports the concept that IRP action occurs over a regulatory continuum that ranges from weakest (*Aco2*) to strongest (*Fth1* and *Ftl*) targets. That IRPs are significant determinants of this hierarchy is supported by the range of affinities of IRP1 for natural 5' IREs which reflects the translational hierarchy observed here and the relationship between IRE mutations in HHCS and the impact of IRP1 and IRP2 binding affinities (16,19). Second, the hierarchical control of IRE-containing mRNA generates a regulatory landscape where some targets of IRP action respond more strongly to iron excess while others respond preferentially to iron deficiency. Our study provides compelling evidence that the mRNA regulon controlled by IRPs is wired in a manner that allows separate but overlapping control of cellular iron metabolism and cellular response to iron deficiency in order to optimize the response to the continuum of iron availability from deficient to excessive.

Coordinate control of mRNA fate through the control of RNA regulons has central roles in cell proliferation, inflammatory responses, cancer and an array of other critical cellular and organismal processes (1,3,4). Our work comparing the iron-dependent control of the fate of 5' IRE-containing mRNAs supports the concept of separate regulatory groups within this RNA regulon. At

the translational level a first-line defense against iron-induced oxidative stress is exhibited by the FTH1 and FTL subunits and FPN1. These three mRNAs are most strongly translationally repressed in iron-sufficient cells and consequently respond most robustly to iron excess through a substantial increase in translation. Thus, coordinated high-level production of these proteins when iron levels rise lowers the risk of iron-dependent cellular damage by sequestering iron in the assembled ferritin shell and exporting iron via FPN1 which supports the concept that this regulatory group of mRNAs subject to IRP action is one of cellular defense. We suggest that a second regulatory group of mRNA subject to IRP-dependent control of translation involves mRNAs that are weakly targeted including m-acon as analyzed here but also ALAS2 and HIF-2α as examined previously (24,26). These mRNAs encode proteins essential for cell function when iron levels are optimal and whose function need not be strongly increased in iron overload. Instead, these mRNAs encode proteins whose function can be deleterious in iron deficiency. In the case of m-acon, it is well known that iron deficiency leads to impaired expression of iron-containing proteins essential for oxidative phosphorylation and this may be associated with increased formation of oxygen radicals (41). IRP-dependent suppression of m-acon in iron deficiency may limit TCA cycle flux thus reducing the level of oxygen radicals as is the case regarding the control of aconitase

activity in *E. coli (42)*. In the case of ALAS2, suppression of its activity in iron deficiency prevents accumulation of the heme precursor protoporphyrin IX which can be toxic as it is in X-linked dominant protoporphyria in humans or the mild erythropoietic protoporphyria seen in *Irp2*$^{-/-}$ mice (43,44). Lastly, the transcription factor HIF-2α is the primary driver of erythropoietin (Epo) production and other genes critical for the adaptive response to hypoxia. IRP1 deficiency leads to inappropriate levels of Epo and polycythemia (24,45,46). Iron deficiency itself induces a block in erythropoiesis (47) and the failure to suppress Epo production via IRP1-mediated regulation may dysregulate erythropoiesis.

To gain additional insight concerning the mechanism through which 5' IRE-containing mRNA are differentially controlled we determined the dissociation rates of IRP1 with IREs at the extremes of the RNA binding hierarchy, *Ftl1* and *Aco2*. The substantially faster off-rate of IRP1 with the *Aco2* IRE relative to the *Ftl1* IRE suggests increased accessibility of *Aco2* mRNA to the translational initiation machinery as IRPs are predicted to spend less time associated with *Aco2* mRNA. Presumably other 5' IREs that bind weakly to IRPs relative to ferritin mRNA possess a similar translational advantage although differential interaction of these mRNA with translation initiation factors must also be considered (36,48,49). The faster off-rate for the *Aco2* IRE is

consistent with the enhanced translational activity of this mRNA observed in liver under steady state conditions and the reduced response of this messenger to iron deficiency. The faster off-rate predicts a more rapid kinetics of translational activation of *Aco2* mRNA in response to agents that inhibit IRP RNA binding activity. While our previous studies in IRP-deficient mice suggested a preferential role of IRP2 in controlling 5'IRE-containing mRNA other than HIF-2α, we note that the relative proportion of mRNAs remaining in the repressed (RNP) pool in *Irp2*$^{-/-}$ mice was greatest for the ferritin subunits followed by *Fpn1* and *Aco2* mRNA (24). A logical interpretation of these previous results is that the hierarchical differences in K_D and the associated difference in off-rate of IRP1 for 5' IREs is a key determinant of the differentially repression of mRNA in both wildtype as well as *Irp2*$^{-/-}$ mice.

When comparing our studies of the high affinity (picomolar K_D) complex of IRP1 bound to IRE, the fold-difference in K_D across the IRE RNA binding hierarchy of 9-fold (19) exceeds the 6- to 7-fold range in off-rate we report here when comparing L-ferritin and m-acon IRE. The non-equivalence in these values suggests that the association rate of IRP1 in forming the high affinity complex is also different for specific IRE. Previous studies using a fluorescence anisotropy assay to study a lower affinity (nanomolar K_D) IRP1-IRE complex observed a significant impact of IRE

species on the rate of association with IRP1 (48-50). No difference in the off-rate for this low affinity complex was observed (48). Taken together, these studies may suggest that IRP1 binds to IREs to form an initial low affinity unstable complex where the rate of association is a key factor distinguishing different IRE. We propose that then there is transition to the higher affinity (picomolar K_D) complexes that differ in their inherent stability.

Since the discovery of translational control of ferritin expression in the 1960s much effort has focused on unraveling the mechanism and determining the extent to which it represented a commonly used paradigm of gene regulation (51,52). However, it is less well recognized that the original studies on iron regulation of ferritin protein accumulation by Drysdale and Munro demonstrated a substantial and comparable impact of acute iron overload on both the synthesis and degradation of ferritin in rat liver (37). These and subsequent studies revealed that ferritin protein is unstable under iron-deficient conditions which recently has been shown to involve the lysosomal targeting protein NCOA4 (39,53). Our studies reveal a developmental regulation of the relative roles of translational and post-translational mechanisms in dictating the steady state expression of ferritin. In adult rats we observed the classic pattern for control of ferritin expression with a 3-fold reduction in translational activity of *Fth1* and *Ftl* mRNAs that accompanied the 5-fold

impact on ferritin protein level when comparing liver of rats fed the iron deficient versus the iron sufficient diet. In contrast, in weanling rats a substantial 4-fold change in ferritin protein abundance in liver without any change in mRNA translation state was observed in response to dietary iron deficiency. We conclude that translational control is not an obligatory mechanism for iron-dependent control of ferritin expression. Taken together with the key role of hepcidin-dependent control of FPN1 protein degradation (38) it is clear that coordinated modulation of mRNA translation and protein stability act in concert to modulate the ultimate level of expression of proteins encoded by IRE-containing mRNA.

Studies of IRP deficiency established tissue-specific roles of each IRP in critical physiological processes including key aspects of brain function, erythropoiesis, mitochondrial function and intestinal iron absorption (43,45,46,54-60). A more refined understanding of the regulatory breadth of the IRE-IRP regulon is needed in order to fully define its roles not only in normal physiology but also in diseases where iron dysregulation contributes to pathology. Contributors to the phenotypic consequences of IRP dysregulation likely include differences in the tissue-specific expression level of IRE-containing mRNA, the signaling pathways controlling IRP1 versus IRP2 RNA binding activity, and their affinity for natural or mutant IREs (3,16,19,61). Our

finding that 5' IRE-containing mRNAs are hierarchically controlled at the translational level to changes in IRP RNA binding activity, as induced in our study by changes in iron status, predicts that the specific aspects of iron metabolism contributing to disease etiology will depend on whether IRP action is diminished or enhanced. Thus, loss of IRE RNA binding activity likely induces an iron-deficiency phenotype due to enhanced iron storage and export. In contrast, activation of IRPs would be associated with maladaptive increases in cellular iron accumulation with insufficient storage, impairment of the hypoxia response or impaired energy metabolism. Given the evidence that both canonical and putative non-canonical IREs are found in mRNAs encoding proteins without clear roles in iron metabolism additional regulatory groups of mRNA controlled by IRP action are yet to be elucidated (9,14,62,63).

CONCLUSIONS:

Hierarchical translational control of 5' IRE-containing mRNA involves a graded response to changes in animal cell iron status. mRNAs encoding iron storage or export proteins are the most tightly controlled by IRPs. In liver of rats fed an iron sufficient diet these mRNAs encoding proteins required for iron sequestration or export are largely translationally repressed and consequently

respond most robustly to excessive levels of iron. In contrast, mRNAs encoding proteins involved in cellular iron utilization or the adaptive responses to iron deficiency are actively translated in liver of rats fed an iron sufficient diet, show only a small response to iron overload, and are most strongly affected by iron deficiency. Differences in the iron-dependent setpoint modulating these two phases of translational regulation is central to the proper maintenance of cellular iron metabolism and viability.

CONFLICTS OF INTEREST

There are no conflicts to declare.

ACKNOWLEDGEMENTS

We thank Dan Steffen for preparing [^{32}P]RNA for gel shifts and Prof. M. Thomas Record for advice on off-rate assays. This work was supported in part by NIH R01 DK66600 and USDA Hatch grant accession number 1014006 to RSE. We thank Kathryn Deck for excellent editorial assistance.

FOOTNOTES

[a] Associate Scientific Director, MediTech Media, Two Ravinia Drive, Suite 605, Atlanta, GA 30346

[b] Department of Nutritional Sciences, 301 HS, Oklahoma State University, Stillwater, OK 74078

[c] Hologic Inc., 10210 Genetic Center Drive, San Diego, CA 92121

[d] Exploration Academy, 400 N. Main St. Verona, WI. 53593

[e] AbbVie Pharmacogenetics, Genomics Research Center, AP31-1 Room 01P14C, 1 N. Waukegan Road,

North Chicago, IL. 60064

[†] These authors contributed equally.

REFERENCES

1. Bisogno, L. S., and Keene, J. D. (2017) RNA regulons in cancer and inflammation. *Curr Opin Genet Dev* **48**, 97-103
2. McCown, P. J., Corbino, K. A., Stav, S., Sherlock, M. E., and Breaker, R. R. (2017) Riboswitch diversity and distribution. *RNA* **23**, 995-1011
3. Muckenthaler, M. U., Rivella, S., Hentze, M. W., and Galy, B. (2017) A Red Carpet for Iron Metabolism. *Cell* **168**, 344-361
4. Prasad, A., Porter, D. F., Kroll-Conner, P. L., Mohanty, I., Ryan, A. R., Crittenden, S. L., Wickens, M., and Kimble, J. (2016) The PUF binding landscape in metazoan germ cells. *RNA* **22**, 1026-1043
5. Anderson, C. P., Shen, M., Eisenstein, R. S., and Leibold, E. A. (2012) Mammalian iron metabolism and its control by iron regulatory proteins. *Biochim Biophys Acta* **1823**, 1468-1483
6. Gray, N. K., and Hentze, M. W. (1994) Iron regulatory protein prevents binding of the 43S translation pre-initiation complex to ferritin and eALAS mRNAs. *EMBO J.* **13**, 3882-3891
7. Cho, H. H., Cahill, C. M., Vanderburg, C. R., Scherzer, C. R., Wang, B., Huang, X., and Rogers, J. T. (2010) Selective translational control of the Alzheimer amyloid precursor protein transcript by iron regulatory protein-1. *J Biol Chem* **285**, 31217-31232
8. Luscieti, S., Galy, B., Gutierrez, L., Reinke, M., Couso, J., Shvartsman, M., Di Pascale, A., Witke, W., Hentze, M. W., Pilo Boyl, P., and Sanchez, M. (2017) The actin-binding protein profilin 2 is a novel regulator of iron homeostasis. *Blood* **130**, 1934-1945
9. Sanchez, M., Galy, B., Schwanhaeusser, B., Blake, J., Bahr-Ivacevic, T., Benes, V., Selbach, M., Muckenthaler, M. U., and Hentze, M. W. (2011) Iron regulatory protein-1 and -2: transcriptome-wide definition of binding mRNAs and shaping of the cellular proteome by iron regulatory proteins. *Blood* **118**, e168-179
10. dos Santos, C. O., Dore, L. C., Valentine, E., Shelat, S. G., Hardison, R. C., Ghosh, M., Wang, W., Eisenstein, R. S., Costa, F. F., and Weiss, M. J. (2008) An iron responsive element-like stem-loop regulates alpha-hemoglobin-stabilizing protein mRNA. *J Biol Chem* **283**, 26956-26964

11. Theil, E. C., and Goss, D. J. (2009) Living with iron (and oxygen): questions and answers about iron homeostasis. *Chemical reviews* **109**, 4568-4579
12. Gray, N. K., Pantopoulos, K., Dandekar, T., Ackrell, B., and Hentze, M. W. (1996) Translational regulation of mammalian and drosophila citric acid cycle enzymes via iron-responsive elements. *Proc. Natl. Acad. Sci. USA* **93**, 4925-4930
13. Kim, H.-Y., LaVaute, T., Iwai, K., Klausner, R. D., and Rouault, T. A. (1996) Identification of a conserved and functional iron-responsive element in the 5'-untranslated region of mammalian mitochondrial aconitase. *J. Biol. Chem.* **271**, 24226–24230
14. Sanchez, M., Galy, B., Dandekar, T., Bengert, P., Vainshtein, Y., Stolte, J., Muckenthaler, M. U., and Hentze, M. W. (2006) Iron regulation and the cell cycle: identification of an iron-responsive element in the 3'-untranslated region of human cell division cycle 14A mRNA by a refined microarray-based screening strategy. *J Biol Chem* **281**, 22865-22874
15. Sanchez, M., Galy, B., Muckenthaler, M. U., and Hentze, M. W. (2007) Iron-regulatory proteins limit hypoxia-inducible factor-2alpha expression in iron deficiency. *Nat Struct Mol Biol* **14**, 420-426
16. Allerson, C. R., Cazzola, M., and Rouault, T. A. (1999) Clinical severity and thermodynamic effects of iron-responsive element mutations in hereditary hyperferritinemia-cataract syndrome. *J. Biol. Chem.* **274**, 26439-26447
17. Beaumont, C., Leneuve, P., Devaux, I., Scoazec, J.-Y., Berthier, M., Loiseau, M.-N., Grandchamp, B., and Bonneau, D. (1995) Mutation in the iron responsive element of the L ferritin mRNA in a family with dominant hyperferritinaemia and cataract. *Nature Genet.* **11**, 444-446
18. Luscieti, S., Tolle, G., Aranda, J., Campos, C. B., Risse, F., Moran, E., Muckenthaler, M. U., and Sanchez, M. (2013) Novel mutations in the ferritin-L iron-responsive element that only mildly impair IRP binding cause hereditary hyperferritinaemia cataract syndrome. *Orphanet journal of rare diseases* **8**, 30
19. Goforth, J. B., Anderson, S. A., Nizzi, C. P., and Eisenstein, R. S. (2010) Multiple determinants within iron-responsive elements dictate iron regulatory protein binding and regulatory hierarchy. *RNA* **16**, 154-169
20. Aziz, N., and Munro., H. N. (1986) Both subunits of rat liver ferritin are regulated at a translational level by iron induction. *Nucl. Acids Res.* **14**, 915-927

21. Rogers, J., and Munro, H. N. (1987) Translation of ferritin light and heavy subunit mRNAs is regulated by intracellular chelatable iron levels in rat hepatoma cells. *Proceedings of the National Academy of Sciences* **84**, 2277-2281
22. White, K., and Munro, H. N. (1988) Induction of ferritin subunit synthesis by iron is regulated at both the transcriptional and translational levels. *J. Biol. Chem.* **263**, 8938-8942
23. Zahringer, J., Baliga, B. S., and Munro, H. N. (1976) Novel mechanism for translational control in regulation of ferritin synthesis by iron. *Proc. Natl. Acad. Sci. USA* **73**, 857-861
24. Anderson, S. A., Nizzi, C. P., Chang, Y. I., Deck, K. M., Schmidt, P. J., Galy, B., Damnernsawad, A., Broman, A. T., Kendziorski, C., Hentze, M. W., Fleming, M. D., Zhang, J., and Eisenstein, R. S. (2013) The IRP1-HIF-2alpha Axis Coordinates Iron and Oxygen Sensing with Erythropoiesis and Iron Absorption. *Cell metabolism* **17**, 282-290
25. Davis, M. R., Shawron, K. M., Rendina, E., Peterson, S. K., Lucas, E. A., Smith, B. J., and Clarke, S. L. (2011) Hypoxia inducible factor-2 alpha is translationally repressed in response to dietary iron deficiency in Sprague-Dawley rats. *J Nutr* **141**, 1590-1596
26. Schranzhofer, M., Schifrer, M., Cabrera, J. A., Kopp, S., Chiba, P., Beug, H., and Mullner, E. W. (2006) Remodeling the regulation of iron metabolism during erythroid differentiation to ensure efficient heme biosynthesis. *Blood* **107**, 4159-4167
27. Kim, H. D., Nienhaus, G. U., Ha, T., Orr, J. W., Williamson, J. R., and Chu, S. (2002) Mg^{2+}-dependent conformational change of RNA studied by fluorescence correlation and FRET on immobilized single molecules. *Proc. Natl. Acad. Sci. USA* **99**, 4284-4289
28. Anthony, T. G., Anthony, J. C., Yoshizawa, F., Kimball, S. R., and Jefferson, L. S. (2001) Oral administration of leucine stimulates ribosomal protein mRNA translation but not global rates of protein synthesis in the liver of rats. *J. Nutr.* **131**
29. Chen, O. S., Schalinske, K. L., and Eisenstein, R. S. (1997) Dietary iron intake modulates the activity of iron regulatory proteins (IRPs) and the abundance of ferritin and mitochondrial aconitase in rat liver. *J. Nutr.* **127**, 238-248
30. van-Kampen, E. J., and Zijlstra, W. G. (1961) Standardization of hemoglobinometry II. The hemoglobincyanide method. *Clin. Chim. Acta* **6**, 538-544
31. Barton, H. A., Eisenstein, R. S., Bomford, A. B., and Munro, H. N. (1990) Determinants of the interaction of the iron regulatory element binding protein with its binding site in rat L-ferritin mRNA. *J. Biol. Chem.* **265**, 7000-7008

32. Hanson, E. S., and Leibold, E. A. (1998) Regulation of iron regulatory protein 1 during hypoxia and hypoxia/reoxygenation. *J. Biol. Chem.* **273**, 7588-7593
33. Hanson, E. S., Rawlins, M. L., and Leibold, E. A. (2003) Oxygen and iron regulation of iron regulatory protein 2. *J. Biol. Chem.* **278**, 40337-40342
34. Salahudeen, A. A., Thompson, J. W., Ruiz, J. C., Ma, H. W., Kinch, L. N., Li, Q., Grishin, N. V., and Bruick, R. K. (2009) An E3 Ligase Possessing an Iron Responsive Hemerythrin Domain Is a Regulator of Iron Homeostasis. *Science* **326**, 722-726
35. Vashisht, A. A., Zumbrennen, K. B., Huang, X., Powers, D. N., Durazo, A., Sun, D., Bhaskaran, N., Persson, A., Uhlen, M., Sangfelt, O., Spruck, C., Leibold, E. A., and Wohlschlegel, J. A. (2009) Control of Iron Homeostasis by an Iron-Regulated Ubiquitin Ligase. *Science* **326**, 718-721
36. Khan, M. A., Walden, W. E., Goss, D. J., and Theil, E. C. (2009) Direct Fe2+ sensing by iron responsive messenger RNA/repressor complexes weakens binding. *J Biol Chem*
37. Drysdale, J. W., and Munro, H. N. (1966) Regulation of synthesis and turnover of ferritin in rat liver. *J. Biol. Chem.* **241**, 3630-3637
38. Nemeth, E., Tuttle, M. S., Powelson, J., Vaughn, M. B., Donovan, A., Ward, D. M., Ganz, T., and Kaplan, J. (2004) Hepcidin regulates cellular iron efflux by binding to ferroportin and inducing its internalization. *Science* **306**, 2090-2093
39. Truty, J., Malpe, R., and Linder, M. C. (2001) Iron prevents ferritin turnover in hepatic cells. *J. Biol. Chem.* **276**, 48775-48780
40. Mancias, J. D., Wang, X., Gygi, S. P., Harper, J. W., and Kimmelman, A. C. (2014) Quantitative proteomics identifies NCOA4 as the cargo receptor mediating ferritinophagy. *Nature* **509**, 105-109
41. Cartier, L.-J., Ohira, Y., Chen, M., Cuddihee, R. W., and Holloszy, J. O. (1986) Perturbation of mitochondrial composition in muscle by iron deficiency. *J. Biol. Chem.* **261**, 13827-13832
42. Gardner, P. R. (1997) Superoxide-driven aconitase Fe-S center cycling. *Biosci. Reports* **17**, 33-42
43. Cooperman, S. S., Meyron-Holtz, E. G., Olivierre-Wilson, H., Ghosh, M. C., McConnell, J. P., and Rouault, T. A. (2005) Microcytic anemia, erythropoietic protoporphyria, and neurodegeneration in mice with targeted deletion of iron-regulatory protein 2. *Blood* **106**, 1084-1091

44. Puy, H., Gouya, L., and Deybach, J. C. (2010) Porphyrias. *Lancet* **375**, 924-937

45. Ghosh, M. C., Zhang, D. L., Jeong, S. Y., Kovtunovych, G., Ollivierre-Wilson, H., Noguchi, A., Tu, T., Senecal, T., Robinson, G., Crooks, D. R., Tong, W. H., Ramaswamy, K., Singh, A., Graham, B. B., Tuder, R. M., Yu, Z. X., Eckhaus, M., Lee, J., Springer, D. A., and Rouault, T. A. (2013) Deletion of Iron Regulatory Protein 1 Causes Polycythemia and Pulmonary Hypertension in Mice through Translational Derepression of HIF2alpha. *Cell metabolism* **17**, 271-281

46. Wilkinson, N., and Pantopoulos, K. (2013) IRP1 regulates erythropoiesis and systemic iron homeostasis by controlling HIF2alpha mRNA translation. *Blood* **122**, 1658-1668

47. Bullock, G. C., Delehanty, L. L., Talbot, A. L., Gonias, S. L., Tong, W. H., Rouault, T. A., Dewar, B., Macdonald, J. M., Chruma, J. J., and Goldfarb, A. N. (2010) Iron control of erythroid development by a novel aconitase-associated regulatory pathway. *Blood* **116**, 97-108

48. Khan, M. A., Ma, J., Walden, W. E., Merrick, W. C., Theil, E. C., and Goss, D. J. (2014) Rapid kinetics of iron responsive element (IRE) RNA/iron regulatory protein 1 and IRE-RNA/eIF4F complexes respond differently to metal ions. *Nucleic Acids Res* **42**, 6567-6577

49. Khan, M. A., Walden, W. E., Theil, E. C., and Goss, D. J. (2017) Thermodynamic and Kinetic Analyses of Iron Response Element (IRE)-mRNA Binding to Iron Regulatory Protein, IRP1. *Sci Rep* **7**, 8532

50. Ma, J., Haldar, S., Khan, M. A., Sharma, S. D., Merrick, W. C., Theil, E. C., and Goss, D. J. (2012) Fe2+ binds iron responsive element-RNA, selectively changing protein-binding affinities and regulating mRNA repression and activation. *Proc Natl Acad Sci U S A* **109**, 8417-8422

51. Drysdale, J. W., and Munro, H. N. (1965) Failure of Actinomycin D to Prevent Induction of Liver Apoferritin after Iron Administration. *Biochim Biophys Acta* **103**, 185-188

52. Saddi, R., and von der Decken, A. (1965) The effect of iron administration on the incorporation of [14C] leucine into ferritin by rat-liver systems. *Biochim Biophys Acta* **111**, 124-133

53. Santana-Codina, N., and Mancias, J. D. (2018) The Role of NCOA4-Mediated Ferritinophagy in Health and Disease. *Pharmaceuticals (Basel)* **11**

54. Galy, B., Ferring, D., Minana, B., Bell, O., Janser, H. G., Muckenthaler, M., Schumann, K., and Hentze, M. W. (2005) Altered body iron distribution and microcytosis in mice deficient in iron regulatory protein 2 (IRP2). *Blood* **106**, 2580-2589

55. Galy, B., Ferring-Appel, D., Becker, C., Gretz, N., Grone, H. J., Schumann, K., and Hentze, M. W. (2013) Iron regulatory proteins control a mucosal block to intestinal iron absorption. *Cell reports* **3**, 844-857

56. Galy, B., Ferring-Appel, D., Kaden, S., Grone, H. J., and Hentze, M. W. (2008) Iron regulatory proteins are essential for intestinal function and control key iron absorption molecules in the duodenum. *Cell metabolism* **7**, 79-85

57. Galy, B., Ferring-Appel, D., Sauer, S. W., Kaden, S., Lyoumi, S., Puy, H., Kolker, S., Grone, H. J., and Hentze, M. W. (2010) Iron regulatory proteins secure mitochondrial iron sufficiency and function. *Cell metabolism* **12**, 194-201

58. Ghosh, M. C., Tong, W. H., Zhang, D., Ollivierre-Wilson, H., Singh, A., Krishna, M. C., Mitchell, J. B., and Rouault, T. A. (2008) Tempol-mediated activation of latent iron regulatory protein activity prevents symptoms of neurodegenerative disease in IRP2 knockout mice. *Proc Natl Acad Sci U S A* **105**, 12028-12033

59. LaVaute, T., Smith, S., Cooperman, S., Iwai, K., Land, W., Meyron-Holtz, E., Drake, S. K., Miller, G., Abu-Asab, M., Tsokos, M., 3rd, R. S., Grinberg, A., Love, P., Tresser, N., and Roault, T. A. (2001) Targeted deletion of the gene encoding iron regulatory protein-2 causes misregulation of iron metabolism and neurodegenrative disease in mice. *Nature Genet.* **27**, 209-214.

60. Martelli, A., Schmucker, S., Reutenauer, L., Mathieu, J. R., Peyssonnaux, C., Karim, Z., Puy, H., Galy, B., Hentze, M. W., and Puccio, H. (2015) Iron regulatory protein 1 sustains mitochondrial iron loading and function in frataxin deficiency. *Cell metabolism* **21**, 311-322

61. Stys, A., Galy, B., Starzynski, R. R., Smuda, E., Drapier, J. C., Lipinski, P., and Bouton, C. (2011) Iron regulatory protein 1 outcompetes iron regulatory protein 2 in regulating cellular iron homeostasis in response to nitric oxide. *J Biol Chem* **286**, 22846-22854

62. Cmejla, R., Petrak, J., and Cmejlova, J. (2006) A novel iron responsive element in the 3'UTR of human MRCKalpha. *Biochem Biophys Res Commun* **341**, 158-166

63. Dandekar, T., Stripecke, R., Gray, N. K., Goossen, R., Constable, A., H.E., J., and Hentze, W. (1991) Identification of a novel IRE in murine and human eALAS mRNA. *EMBO J.* **10**, 1903-1909

Table 1. Selective Translational Regulation of 5′ IRE-Containing mRNA in Adult Rat Liver

		Percent Total mRNA in Fraction[1]		
mRNA	Treatment	RNP	40S/60S/80S	Polysomes
Tth	AC	9.9 ± 2.6	6.3 ± 1.2	83.8 ± 3.2
	FAC	5.8 ± 2.2	6.3 ± 0.9	87.9 ± 1.8
Cs	AC	11.2 ± 1.8	13.7 ± 0.6	75.1 ± 2.0
	FAC	6.3 ± 2.8	17.9 ± 1.9	75.8 ± 1.7
Ftl	AC	75.7 ± 4.9[a]	12.3 ± 4.3 [a]	12.0 ± 1.6[a]
	FAC	12.5 ± 2.8[b]	5.1 ± 1.1 [b]	82.4 ± 2.8[b]
Fth1	AC	79.7 ± 4.0 [a]	8.1 ± 4.0 [a]	12.2 ± 1.2 [a]
	FAC	15.0 ± 2.6 [b]	4.2 ± 1.3 [b]	80.8 ± 2.8 [b]
Fpn1	AC	72.9 ± 1.7 [a]	9.4 ± 0.3 [a]	17.8 ± 1.4a [a]
	FAC	12.3 ± 1.8 [b]	4.5 ± 0.6 [b]	86.2 ± 1.8 [b]
Aco2	AC	23.2 ± 5.5[a]	14.5 ± 1.1[a]	62.3 ± 4.4[a]

	FAC	2.9 ± 1.6[b]	13.3 ± 1.0[b]	83.9 ± 2.6[b]

[1] The RNA content of gradient fractions was determined by real time RT PCR as described in Methods. Different superscripts between rows denote statistically significant differences between control rats treated with ammonium citrate (AC) or rats acutely iron-overloaded with ferric ammonium citrate (FAC) for individual mRNA, $p < 0.05$. Values are expressed as mean ± SEM (n = 3).

[2] Rats were injected with ammonium citrate as a control (AC) or with ferric ammonium citrate to induce iron overload (see Methods). Samples were analyzed 3 hr after injection.

Table 2. Differential Impact of Iron Deficiency on Translational Repression of 5′ IRE-Containing mRNA in Adult Rat Liver

			Percent Total Gradient mRNA in Fraction[1]		
mRNA	Diet[2]	Total mRNA[3]	RNP	40S/60S/80S	Polysomes
Tth	C	492 ± 62[a]	15.1 ± 4.7	6.9 ± 0.8	78.0 ± 5.3
	ID	153 ± 34[b]	10.1 ± 2.4	6.7 ± 1.2	83.1 ± 2.8
Cs	C	328 ± 20[a]	11.1 ± 2.4	17.7 ± 1.6	71.3 ± 2.1
	ID	140 ± 32[b]	12.1 ± 1.4	21.6 ± 1.2	66.3 ± 1.6
Ftl	C	419 ± 48[a]	75.2 ± 5.2	12.1 ± 1.3	12.7 ± 4.2[c]
	ID	131 ± 27[b]	86.7 ± 3.0	8.9 ± 2.7	4.4 ± 0.5[d]
Fpn1	C	349 ± 29[a]	57.3 ± 6.0	11.4 ± 1.7	31.6 ± 4.6 [c]
	ID	237 ± 37[b]	65.0 ± 7.5	18.9 ± 5.1	16.5 ± 2.7 [d]
Aco2	C	156 ± 18[a]	14.5 ± 5.1[c]	11.8 ± 2.3	73.8 ± 7.4[c]
	ID	122 ± 11[a]	42.6 ± 4.8[d]	20.2 ± 4.0	37.2 ± 3.8[d]

[1] The RNA content of gradient fractions was determined by qPCR as described in Methods.

Different superscripts between rows denote statistically significant differences between control (C) and iron deficient (ID) rats for individual mRNA, $p < 0.05$. Values are expressed as mean ± SEM for n = 3 rats for the control group and n=4 rats for the iron-deficient group. TfR1 mRNA concentration increased by 2.8 fold in iron-deficient (766 ± 169) vs. control (271 ± 38) liver ($p < 0.05$).

[2] Rats were fed the control (C) diet for two weeks to increase their iron stores. Then they were fed either the C or iron-deficient (ID) diets for an additional 13 or 14 days (see Methods).

[3] Total mRNA content in liver was determined by real time RT PCR as described in Methods. Results were normalized to the level of expression of 18S rRNA in each sample. RNA concentration is on a relative basis and cannot be compared across mRNA (see Methods).

Table 3. Kinetics of Dissociation of IREs from IRP1[a]

	EMSA		Filter Binding	
RNA	$t_{1/2}$ (min)	k_{-1} (min^{-1})	$t_{1/2}$ (min)	k_{-1} (min^{-1})
Ftl	42.7 ± 7.9	0.019 ± 0.0029	92.1 ± 10.2	0.0083 ± 0.0013
Aco2	5.7 ± 0.8[b]	0.13 ± 0.016[c]	16.7 ± 3.5[d]	0.070 ± 0.020[e]

[a]For the EMSA and filter binding analyses of L-ferritin seven separate experiments were performed. For m-acon six separate EMSA and eleven separate filter binding experiments were used. Results are reported as mean ± SEM.

[b]Significantly different versus L-ferritin (P = 0.0013).

[c]Significantly different versus L-ferritin (P = 0.0001).

[d]Significantly different versus L-ferritin (P = 0.0077).

[e]Significantly different versus L-ferritin (P = 0.0272).

Table 4. Ferritin mRNA Translation is Fully Repressed Irrespective of Iron Status in Weanling Rat Liver

			Percent Total Gradient mRNA in Fraction[1]		
mRNA	Diet[2]	Total mRNA[3]	RNP	40S/60S/80S	Polysomes
Tth	C	320 ± 97	4.7 ± 0.5	5.6 ± 0.9	89.7 ± 1.3
	ID	278 ± 42	4.4 ± 1.1	4.3 ± 1.3	91.3 ± 2.2
Cs	C	350 ± 113	7.5 ± 0.9	13.4 ± 2.4	79.1 ± 3.2
	ID	291 ± 44	9.8 ± 2.6	12.2 ± 2.4	77.9 ± 4.9
Ftl	C	240 ± 79	77.9 ± 1.7	12.0 ± 1.6	10.1 ± 2.6
	ID	199 ± 10	76.7 ± 5.1	15.4 ± 3.6	8.0 ± 1.9
Fpn1	C	515 ± 165	60.7	10.8	28.5
	ID	460 ± 90	63.8	20.8	17.1
Aco2	C	214 ± 60	12.4 ± 3.2[a]	15.6 ± 1.9[a]	72.0 ± 4.8[a]
	ID	265 ± 62	30.9 ± 1.9[b]	23.5 ± 1.7[b]	45.6 ± 3.5[b]

[1] The RNA content of gradient fractions was determined by real time RT PCR as described in Methods. Different superscripts between rows denote statistically significant differences between control (C) and iron deficient (ID) rats for individual mRNA, $p < 0.05$. Values are expressed as mean ± SEM for n = 3 rats. The concentration of *Tfrc* mRNA increased by 6.2-fold in iron-deficient (1161 ± 162) vs control (188 ± 21) liver ($p < 0.05$).

[2] Rats were fed the control (C) or iron-deficient (ID) diets for seven to nine days (see Methods).

[3] Total mRNA content in liver was determined by real time RT PCR as described in Methods. Results were normalized to the level of expression of 18S rRNA in each sample. RNA concentration is on a relative basis and cannot be compared across mRNA (see Methods).

[4] For this study one sample of the C and one from the ID failed during polysome analysis so the average of n = 2 samples/condition is reported. RNA analyses had n = 3.

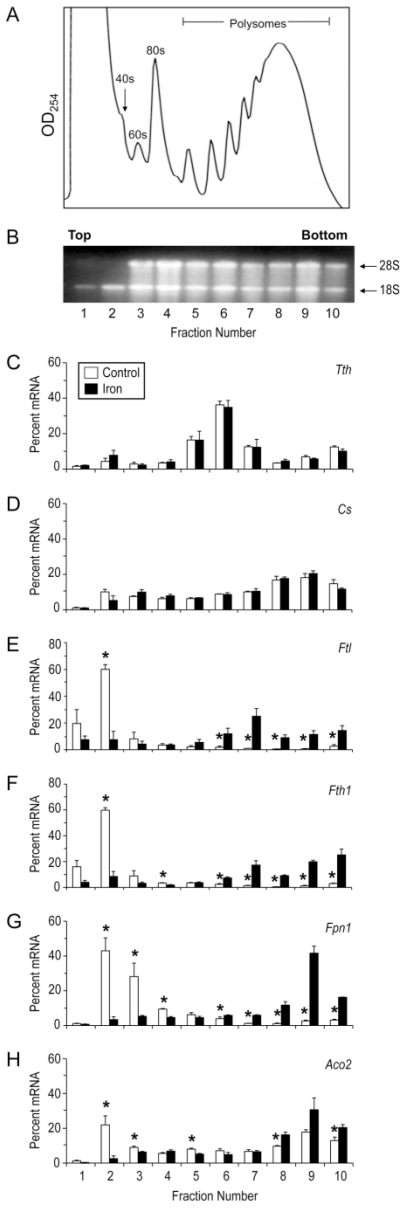

Figure 1: Translation State of 5′ IRE-Containing mRNA in Control and Acutely Iron Overloaded Rat Liver. Adult male rats were intraperitoneally injected with 6 mg of either ammonium citrate (Control) or ferric ammonium citrate (Iron). Polysome profile analysis was performed using liver post-mitochondrial supernatants separated on a sucrose gradient. The gradient was divided into 10 fractions of equal volume from which total RNA was isolated and analyzed by qPCR. A. Optical density at 254 nm, continuously monitored from the top (left) to the bottom (right) of the gradient. B. Agarose gel showing RNA from gradient fractions. Fractions 1-2 contain the free protein pool, some of the messenger ribonucleoprotein pool and some of the 40S ribosomal subunit. Fractions 3-4 contain RNPs, the ribosomal subunits and 80 S monosome, and fractions 5-10 contain the light and heavy polysomes. C.-H. Results of qPCR showing the distribution of the following mRNAs across the gradients: C. transthyretin (Tth); D. citrate synthase (CS); E. L-ferritin (L-Ftn); F. H-ferritin (H-Ftn); G. Ferroportin (Fpn); and H. mitochondrial aconitase (m-Acon). Results are expressed as mean ± standard error of the mean for n = 3 rats per group. An asterisk indicates significantly different from control, $P < 0.05$. See Table 1 for quantification of results.

76x231mm (300 x 300 DPI)

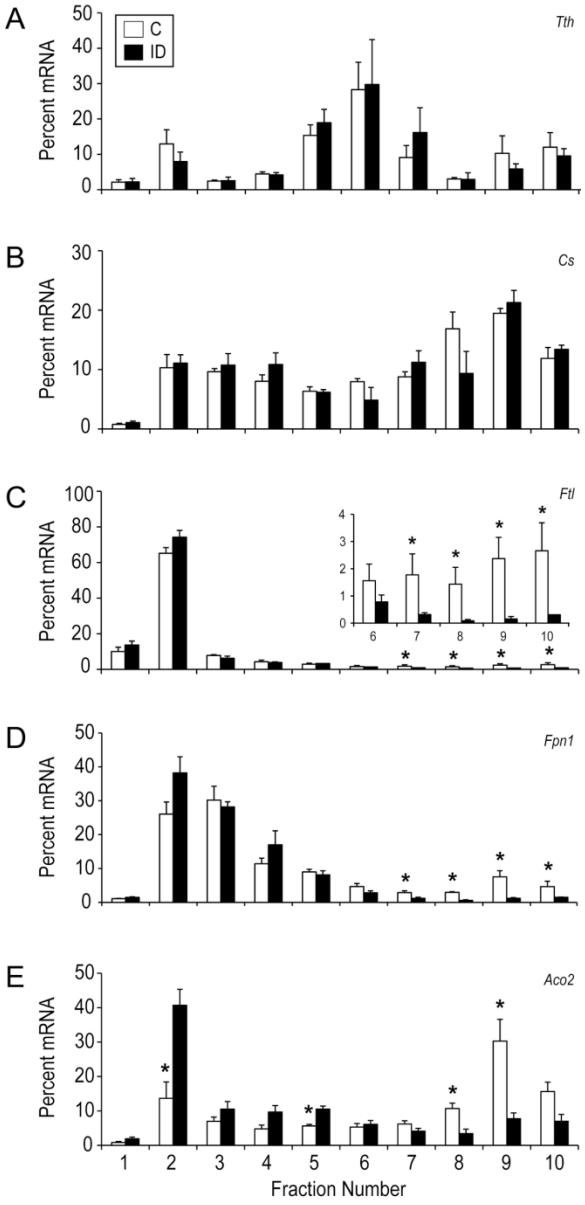

Figure 2: Impact of Iron Deficiency Without Anemia on the Translation State of 5′ IRE-Containing mRNA in Liver. Weanling male Sprague-Dawley rats were fed an iron-adequate control (C) diet for two weeks (see Methods). They were then switched to either an iron-deficient (ID) diet (< 2 ppm iron) or they remained in the control group that received the iron adequate diet for an additional 2 weeks. Polysome profiles of rat liver were generated as described in Methods. A.- E. Results of qPCR showing the distribution of the following mRNAs across the gradients: A. transthyretin (Tth); B. citrate synthase (CS); C. L-ferritin (L-Ftn); D. Ferroportin (Fpn); and E. mitochondrial aconitase (m-Acon). Results are expressed as mean ± standard error of the mean for n = 3 rats per group. An asterisk indicates significantly different from control, P < 0.05. See Table 2 for quantification of results.

96x201mm (300 x 300 DPI)

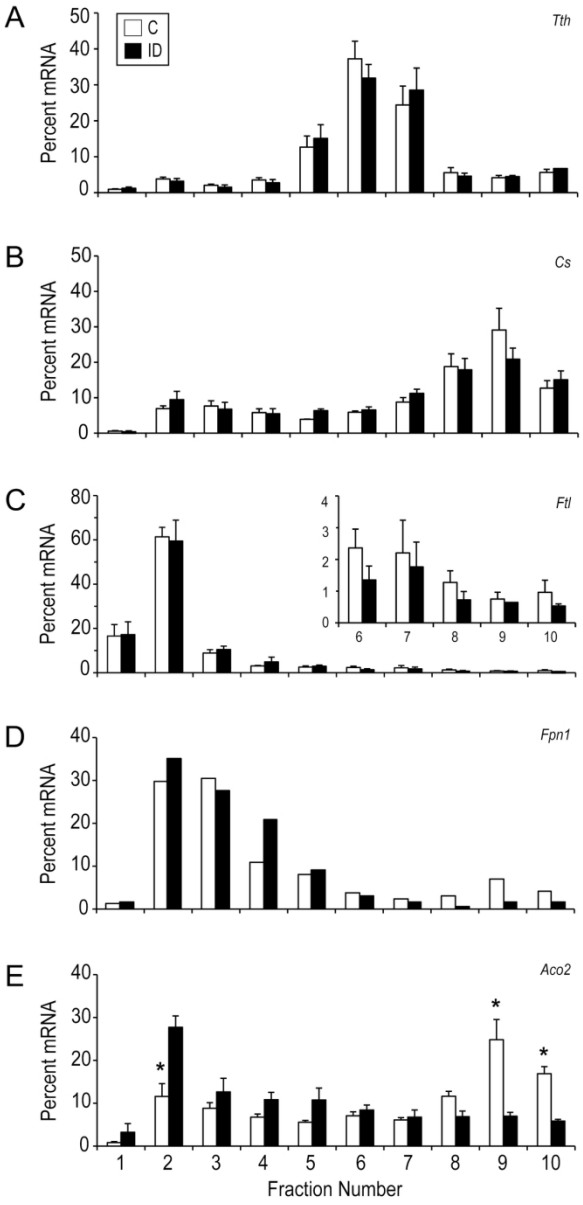

Figure 3: Differential Effect of Iron Deficiency on the Abundance of Liver Proteins Encoded by 5' IRE-Containing mRNA. Liver homogenates from the control and iron deficient rats described in Figure 2 were subjected to immunoblotting to determine the abundance of m-acon and ferritin protein as described in Methods. A. Results as quantified by densitometry. B. representative immunoblots. The SDS-PAGE conditions used did not permit separation of the H- and L-ferritin subunits. Results are expressed as mean ± standard error of the mean for n = 4 rats per group. An asterisk indicates significantly different from control, $P < 0.05$.

97x201mm (300 x 300 DPI)

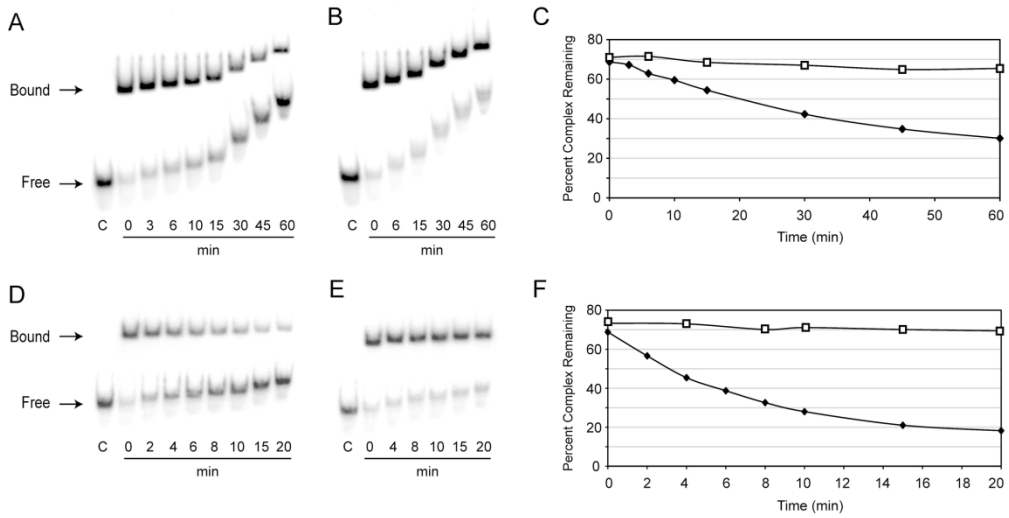

Figure 4: Kinetics of Dissociation of Ferritin and m-Acon IRE from IRP1. Recombinant IRP1 was incubated with either [32P]L-ferritin IRE (A.-C.) or the [32P]m-acon IRE (D.-F.) to form an RNA protein complex at 30 °C. After 10 min a 200-fold excess of unlabeled cognate (filled symbols) or non-cognate (open symbols) RNA was added to the reaction mixture. At indicated time points, samples were mixed with heparin and loaded on an EMSA gel at 4°C. Images of EMSA gels are shown in A.-B., D.-E., with lane numbers indicated below each gel image.: A. EMSA with labeled L-ferritin IRE with unlabeled L-Ft competitor RNA, B. EMSA with labeled L-Ft IRE with unlabeled non-cognate RNA; D. EMSA with labeled m-acon IRE with unlabeled m-acon competitor RNA; E. EMSA with labeled m-Acon IRE with unlabeled non-cognate RNA. Quantified EMSA results are shown in C. and F. for L-Ft and m-acon, respectively. See Table 3 for calculated dissociation rate constants and half-lives, and for results of similar experiments done by filter binding assays.

189x96mm (300 x 300 DPI)

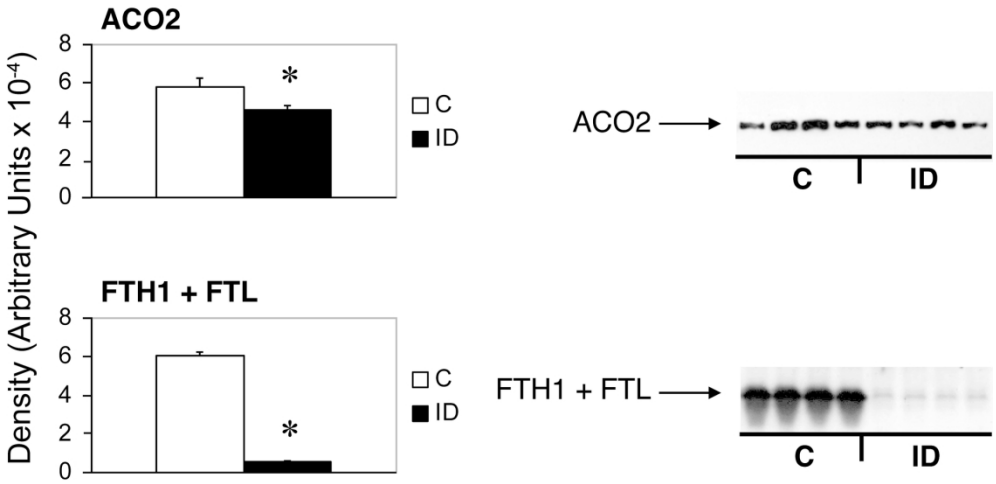

Figure 5: Iron regulation of ferritin protein abundance in the absence of translational regulation. Weanling male Sprague Dawley rats were fed an iron-deficient (ID) diet (< 2 mg Fe/kg diet) or iron adequate (50 mg Fe/kg diet) for 7 to 9 days. Polysome profile analysis was performed as described in Figure 1. A.- E. Results of qPCR showing the distribution of the following mRNAs across the gradients: A. transthyretin (Tth); B. citrate synthase (CS); C. L-ferritin (L-Ftn); D. Ferroportin (Fpn); and E. mitochondrial aconitase (m-Acon). Results are expressed as mean ± standard error of the mean for n = 3 rats per group. An asterisk indicates significantly different from control, $P < 0.05$.

170x81mm (300 x 300 DPI)

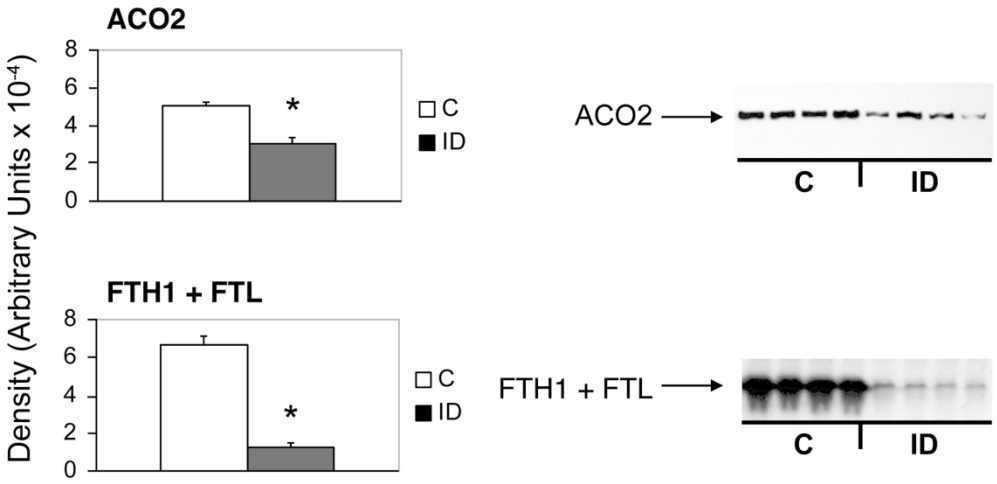

Figure 6: Ferritin Protein Accumulation is Iron Regulated in the Absence of Translational Regulation in Weanling Rat Liver. Liver homogenates from the control and iron deficient rats described in Figure 5 were subjected to immunoblotting to determine the abundance of m-acon and ferritin protein as described in Methods. A. Results as quantified by densitometry. B. Representative immunoblots. The SDS-PAGE conditions used did not permit separation of the H- and L-ferritin subunits. Results are expressed as mean ± standard error of the mean for n = 4 rats per group. An asterisk indicates significantly different from control, $P < 0.05$.

171x82mm (300 x 300 DPI)